Journal of Food Engineering 232 (2018) 56–64

Contents lists available at ScienceDirect

Journal of Food Engineering

journal homepage: www.elsevier.com/locate/jfoodeng

Characterization of dough baked via blue laser

Jonathan David Blutinger [a, *], Yorán Meijers [a, b], Peter Yichen Chen [a], Changxi Zheng [a], Eitan Grinspun [a], Hod Lipson [a]

[a] Columbia University, 116th St & Broadway, New York, NY 10027, USA
[b] Wageningen University, 6708 PB Wageningen, The Netherlands

ARTICLE INFO

Article history:
Received 15 December 2017
Received in revised form
16 March 2018
Accepted 24 March 2018
Available online 28 March 2018

Keywords:
Blue diode laser
Baking
Dough
High-resolution heating
Starch gelatinization
Food layered manufacture

ABSTRACT

Depth of heat penetration and temperature must be precisely controlled to optimize nutritional value, appearance, and taste of food products. These objectives can be achieved with the use of a high-resolution blue diode laser—which operates at 445 nm—by adjusting the water content of the dough and the exposure pattern of the laser. Using our laser, we successfully cooked a 1 mm thick dough sample with a 5 mm diameter ring-shaped cooking pattern, 120 repetitions, 4000 mm min^{-1} speed, and 2 W laser power. Heat penetration in dough products with a blue laser is significantly higher compared to with an infrared laser. The use of a blue laser coupled with an infrared laser yields most optimal cooking conditions for food layered manufacture.

1. Introduction

The heating mechanism used in food layered manufacture (FLM) must be highly controllable and precise to guarantee that a cooked food product meets the taste and appearance requirements (Zoran and Coelho, 2011). The heating mechanism must also accommodate different food shapes and recipe variances, while allowing for custom texturization of food products (Sun et al., 2015). Our laser heating mechanism can be parameterized by a number of variables including speed, power, and spot size, and the heat can be controlled spatially making laser heating ideal for high-resolution food processing. As, to the best of our knowledge, the specific effects of laser wavelength, speed, and power during cooking have not been experimentally studied; this is the objective of the present investigation. Specifically, to explore the effects of a shorter wavelength on the cooking outcomes, we used a blue diode laser that operates at a wavelength of 445 nm, resulting in low water absorbance (Pope and Fry, 1997).

Starch gelatinization is used to assess satisfactory completion of the baking process (Wang and Copeland, 2013). In dough-based products, this phenomenon plays an important role in the transition from raw to baked dough with crumb-like texture, and thus determines product digestibility (Wang and Copeland, 2013; Zanoni et al., 1995a). Starch gelatinization is essential for ensuring that soft baked products have pleasurable appearance and texture (Purlis, 2012). The process begins with starch granules swelling at a temperature in the 60–70 °C range (Olkku and Rha, 1978). With continued heating, starch granules swell and erupt into fragments (Olkku and Rha, 1978). Because this fragmentation occurs on a micron scale, a scanning electron microscope (SEM) can be used to qualitatively assess starch gelatinization (Almeida and Chang, 2013; Huang et al., 1990). Huang et al. (1990) uses SEM to qualitatively characterize changes in potato starch granules during heating. A temperature of 96 °C in the dough core is often used to determine completion of the gelatinization process (Mondal and Datta, 2008; Zanoni et al., 1995b).

Additive manufacturing (AM) technology is a revolutionary way to cook and combine food products. This technology adds layer-upon-layer of material to an object—in this case an edible product—to create complex 3D forms. Some foods that have been printed via this method include chocolate, dough, scallops, meat, sauce, and cheese (Lipton et al., 2015). Combining AM technology with FLM can produce novel food geometries, ingredient combinations not possible with conventional cooking processes, and the

* Corresponding author.
E-mail addresses: jdb2202@columbia.edu (J.D. Blutinger), ymeijers@gmail.com (Y. Meijers), cyc@cs.columbia.edu (P.Y. Chen), cxz@cs.columbia.edu (C. Zheng), eitan@cs.columbia.edu (E. Grinspun), hod.lipson@columbia.edu (H. Lipson).

https://doi.org/10.1016/j.jfoodeng.2018.03.022
0260-8774/

need for high-resolution (millimeter scale) customizable cooking methods for targeted heating of food products (Zoran and Coelho, 2011). Laser beams provide customizable heating favorable in an FLM application since their power, speed, and beam resolution can be precisely controlled digitally (Zoran and Coelho, 2011).

We investigate the applicability of a blue diode laser in dough baking using a simple dough as a food system model. The water content of the dough was altered to determine the effect of degree of saturation on the heating process. Multiple laser-cooking patterns and repeat exposures were used to assess their effects on the temperatures achieved in the dough products. The main objective was to establish the point of complete starch gelatinization in a 1.0 mm thick layer of dough, a common food thickness in FLM.

2. Materials and methods

2.1. Sample preparation

Commercial all-purpose flour (Gold Medal, General Mills, Minneapolis, USA) was used for all experiments involving dough. According to the manufacturer label, 100 g of this flour contains 10 g of protein and 73 g of carbohydrate. The dough was prepared by mixing flour with water (at a 5:3 ratio) in a food processor (FP-8FR series, Cuisinart, East Windsor, USA) for 60 s at low speed in ambient conditions (23 °C). After mixing, the dough was left to rest at 4 °C for at least 15 min. No yeast was added to prevent fermentation and expansion of the dough during storage and further processing. Prior to processing, the dough was laminated into a thickness of 3 mm (±0.1 mm) and square shape with side length 30 mm; only a small portion of this area was treated with a laser (Fig. 3).

2.2. Laser setup

A 3.8 W (445 nm wavelength) blue diode laser (J Tech Photonics, Inc., Kemah, USA) was used for laser cooking. The laser was mounted to a custom acrylic mounting plate that was fastened to the Z-Cart of a vertically mounted screw table, attached to the X Carriage on an X-Carve Gantry (Inventables, Inc., Chicago, USA). To adhere to the health and safety regulations, the apparatus was placed in a custom enclosure made from a 250–520 nm laser shielding acrylic (Fig. 1). Cartesian motion and feed rate—or speed—of the blue laser was controlled by inputting the G-code on an SD card.

The laser power was kept constant at the manufacturer-recommended 2.0 W to avoid overheating and to increase duration of the laser diode operation. The height (the *z* coordinate) is defined as the perpendicular distance between the laser head and the food sample surface. The approximate focal length of the blue laser is 28 mm. Thus, when the height increases above 28 mm the beam diverges, resulting in a larger beam spot size that creates a more diffuse energy profile since the beam is not collimated. Fig. 1 shows an unfiltered dough sample subjected to blue laser processing.

2.3. Laser-cooking patterns

Controlling the laser motion via G-code made it possible to experiment with six different cooking patterns (Fig. 2). Interpolated circular patterns, such as the spiral, ring, and Archimedean spiral (which resulted in a decreased exposure of the sample center), were also explored. However, curved patterns were preferable, since they did not induce significant changes to the laser velocity during scanning. Sharp corners—as opposed to round corners—in a cooking pattern impart a rapid acceleration on the motors in order to maintain a constant velocity, thereby making it difficult to maintain a constant speed throughout the cooking process. The Hilbert curve, a continuous fractal space-filling pattern more commonly used in computer science applications, was also explored, since it offers another efficient means of traversing a 2D dough sample. Moreover, a pattern of interlaced circles was tested to allow for continuity as well as repeated exposure of the sample area.

Images were acquired using a digital single-lens reflex camera (EOS Rebel T5i, Canon, Tokyo, Japan). The images were taken in uncompressed form as a “Canon Raw Version 2” to allow for the highest resolution. Image post-processing was limited to color balancing with a white color swatch, which was placed into the photo-shooting environment. Adobe Photoshop CS6 was used to correct the images.

2.3.1. Calculating energy efficiency

The efficiency of each laser-cooked pattern was estimated by comparing the energy delivered by the laser to the degree of heating exhibited by each cooked dough sample. The following assumptions were made in calculating the efficiency of each pattern: 1) the feed rate remained constant, 2) the laser power remains constant, and 3) the dough was treated as a lumped

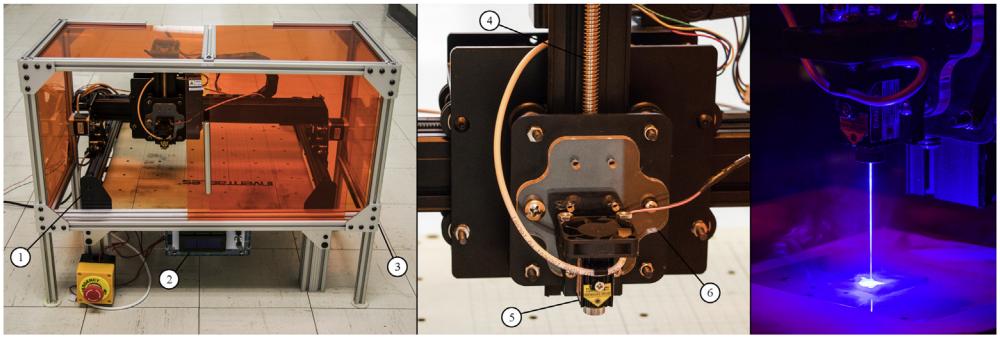

Fig. 1. Experimental setup for the blue diode laser. The diode laser (5) is mounted to the X-Carve gantry (1), which has three degrees of freedom (motion is permitted along the x, y, and z axes, with the latter pertaining to the height above the sample). The apparatus is enclosed in a laser shielding orange acrylic case (3) that has a sliding door that facilitates easy access during experimentation. The optical density of this 250–520 nm laser shielding acrylic is rated at OD 4+. 2: Controller for implementing Gcode, 4: z-axis screw table, 6: custom acrylic mount for diode laser. Right: Dough sample subjected to blue diode laser heating. The beam appears white in the image due to the vibrancy of the light source and camera limitations. The square-shaped dough sample is visible where it comes into contact with the beam and distorts the beam shape. The lack of beam collimation can be observed in this image, as the beam waist occurs just prior to interacting with the dough sample. The contrast and brightness of the image were altered in order to allow the smoke that results from the laser-cooking process to be visualized. (For interpretation of the references to color in this figure legend, the reader is referred to the Web version of this article.)

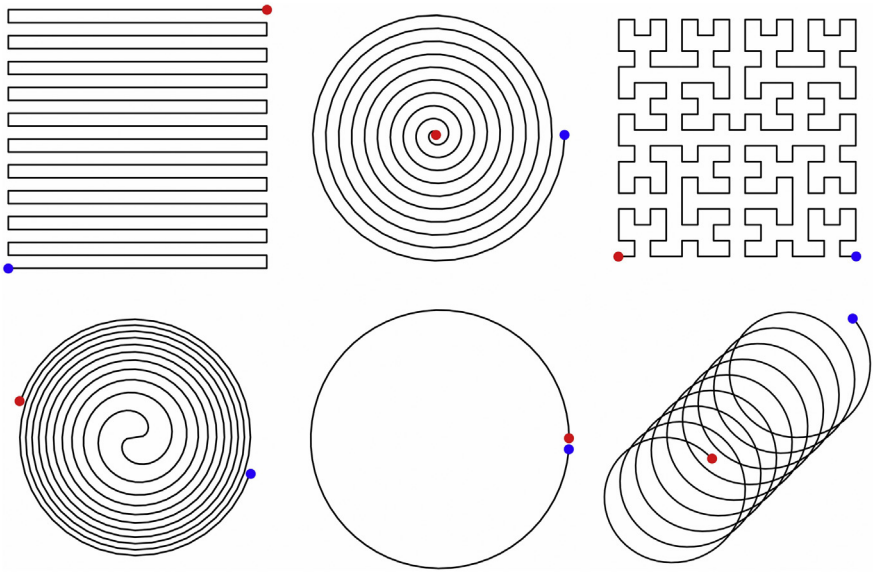

Fig. 2. Cooking patterns applied when using the blue laser. The patterns explored were (from the top left to the bottom right) rectangular raster, spiral, Hilbert curve, Archimedean spiral, ring, and interlaced circles. The red and blue dots represent the start and end points for each cooking pattern. Because the patterns were executed via the X-Carve gantry, corners in the patterns (e.g., rectangular raster and Hilbert curve) caused the machine to decelerate. As this was not the case for curved paths, they were preferable. (For interpretation of the references to color in this figure legend, the reader is referred to the Web version of this article.)

system, as temperature was uniform throughout each dough sample (Wojtkowiak, 2014). The laser energy (E_{laser}) was then calculated as,

$$E_{laser} = P_{laser}t \tag{1}$$

where P_{laser} is laser power (W) and t is the total exposure time of the laser on the dough sample (s). Another way to calculate t is by dividing the total distance traveled by the laser by the feed rate of the laser. The travel distance for the square, rectangle, and interlaced circles cooking patterns are shown in the numerators of Equation (2).

$$t_{raster} = \frac{\left[\frac{wh}{g} + 2h\right]}{v} \tag{2a}$$

$$t_{ic} = \frac{\pi D \rho l}{v} \tag{2b}$$

In Equation (2a) w is width (m), h is height (m), g is the spacing between laser scans (m), and v is the laser feed rate (m s^{-1}), and pertains to the square and rectangle raster patterns, where the scan lines are parallel to w. In Equation (2b), t_{ic} was used to calculate the time required for the interlaced circles pattern (s), where D is the diameter of one of the interlaced circles (m), ρ is the density of circles per unit length (rev m^{-1}), and l is the center-to-center distance from the first to the last interlaced circle (m). The cooking time required for the spiral and Hilbert pattern were computed analytically using MATLAB.

Calculating the degree of dough heating due to laser exposure was determined using the following equation:

$$Q = mc(T_2 - T_1) \tag{3}$$

where Q is the heat energy gained by the dough (W), m is the mass of the dough sample being heated (kg), c is the heat capacity of the dough (J kg^{-1} K^{-1}), T_2 is the averaged maximum temperature at 0.25 mm and 1.0 mm below the surface of the dough (°C), and T_1 is the temperature of the dough prior to heating (°C).

Heating efficiency (η, %) was calculated by dividing the heat energy (Q) by the laser energy (E_{laser}):

$$\eta = \frac{Q}{E_{laser}}. \tag{4}$$

Multiple equations are used to determine energy thresholds for burning in dough cooked by the interlaced circles pattern. Equations (1) and (2b) are used to compute total laser energy (E_{laser}) and Equation (5) is used to calculate the heat-affected area on the dough (A_{ic}, m^2).

$$A_{ic} = D\left(l + \frac{\pi}{4}D\right). \tag{5}$$

Dividing E_{laser} by A_{ic} will yield the total laser energy transfer per unit dough area (ω, J m^{-2}).

2.4. Temperature measurement

The maximum temperature inside the dough samples was recorded with a Leaton 4-Channel K-Type Digital Thermometer Thermocouple Sensors (Shenzhen DeXi Electronics Co, Shenzhen, China) equipped with K-thermocouples (±1 °C), which were inserted at 0.25 and 1.0 mm depth below the dough surface. A depth of 1.0 mm was considered because this is a typical layer height used in food layered manufacture. The measurements were performed in triplicate and—in the pertinent graphs—error bars indicate standard error. The experimental setup is shown in Fig. 3.

2.5. Scanning electron microscopy

The processed sample microstructure was examined under a scanning electron microscope (Sigma VP, Zeiss, Oberkochen, Germany) under the following conditions: high vacuum (pressure below 2×10^{-5} Pa), a working distance of 3.5 mm, and an acceleration voltage of 3 kV. The sample was dried in ambient air and sputter coated with gold prior to analysis.

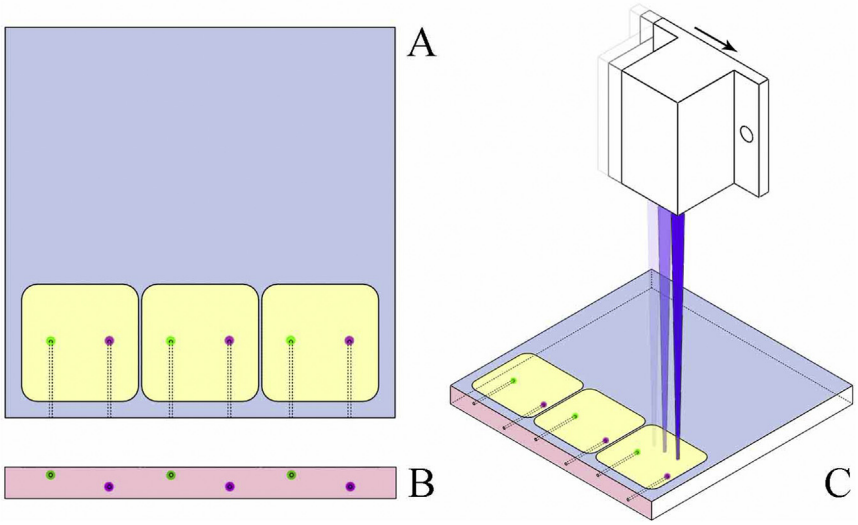

Fig. 3. Setup for measuring internal dough temperature. The isometric view (C) depicts a dough sample, whereas the shaded blue area represents the top view (A), with the side view shown underneath (B). The yellow parts of the image (visible in A and C) indicate the region of the dough that our blue laser passed over irrespective of the cooking pattern. The thermocouples that are 0.25 mm from the surface are shown in green and the sensors that are placed 1.0 mm below the surface are shown in purple. The thermocouples were positioned equidistantly, so that the heat can be absorbed evenly by each thermocouple in the dough sample. The blue laser diode is shown in (C) as it traverses across the surface of one of the cooking areas. (For interpretation of the references to color in this figure legend, the reader is referred to the Web version of this article.)

2.6. Statistical analysis

All of the tests conducted in this study were performed in triplicate to reduce uncertainty. Three sensors were placed in the dough at a depth of 0.25 mm and 1.0 mm. The triplicate measurements were averaged and a standard error was calculated from each set of averaged values by taking the standard deviation of each triplicate data set and dividing it by the square root of three (number of values in the data set). This method of error analysis provides an indication of how similar each measured temperature value is to all other measured temperature values in each data set, with lower errors suggesting more consistent data collection methods. Average and standard error values are displayed in Table 1.

3. Results and discussion

3.1. Effect of dough water content on maximum dough temperature

Because water absorbance at 445 nm is very low (Pope and Fry, 1997), one can posit that water content is an important factor in determining the cooking behavior of dough. The effect of water content on cooking temperature was examined by measuring the temperature at 0.25 and 1.0 mm depth below the dough surface during laser-cooking while varying the water content from 50% to 70% on the flour weight basis (D, Fig. 4). The laser parameters were kept constant in both tests, i.e., the speed of 400 mm min^{-1} power of 2.0 W, and z-height of 58 mm was employed in both cases, corresponding to a beam spot size of approximately 0.5 mm.

The experimental findings indicate that higher internal temperatures were achieved in laser-baked dough samples with greater water content, as the sample with 70% water content was >20% warmer than the sample with 50% water content at both measuring depths (22.6% at 0.25 mm depth and 20.9% at 1.0 mm depth). Maximum temperatures achieved inside the dough samples during the tests are shown in Table 1. This direct correlation between laser-baked dough temperature and dough saturation can be attributed to the low absorbance of water at this wavelength resulting in greater heat penetration depth. Furthermore, surface burning can be observed on the dryer dough sample (D, Fig. 4), which also significantly limits penetration. The burn propagation phenomenon is also visible in these images. As the raster pattern zigzags from the top to the bottom of the image, the burned area gradually increases in width.

3.1.1. Burning propagation

An interesting dough surface burning phenomenon can be observed at high laser energy exposure. Once burning on the dough surface occurs, more energy is absorbed by the dark region, which results in a dramatic decrease in heat transmissivity as compared to uncooked dough. The burnt area will then increase in size and begin to gradually propagate with the laser pattern. As a result of more energy being absorbed by the sample surface, the amount transmitted through the dough is insufficient for cooking to take place. This effect is shown in Fig. 4, where the laser follows an interlaced circles cooking pattern along a counter-clockwise arc.

Due to the low water absorbance at the blue wavelength (445 nm), one can assume that water plays an important role in the cooking behavior of dough when the blue laser is applied. The water content of food products is therefore the key factor in the differences observed when the two laser types are employed.

3.2. Effect of laser pattern on maximum dough temperature

To achieve desirable cooking results, the blue diode laser was subjected to extensive evaluation, varying the key parameters until the optimal values were determined. At the focus height ($z = 0$), the laser beam power density was too concentrated and would cause the sample surface to burn before any heat penetration could occur. To prevent burning, the distance between the laser and the sample (height) was increased, as this resulted in beam dispersion, effectively decreasing power density.

Among the six cooking patterns examined, the interlaced circles were found to be the most effective in terms of heating, as the dough samples were cooked most effectively for three reasons. First, the curved shape of this pattern allows the machine to maintain a constant feed rate during scanning. Second, when the laser moved in overlapping circles, heat could build up very

Table 1
Maximum dough temperatures as a function of recipe, cooking pattern, environmental conditions, and repetitive heating. Each experiment was done in triplicate and the average value and standard error is recorded at each sensor depth within the dough. In the "dough recipe" section, the percentages are on a flour weight basis, and both samples were cooked using a square raster pattern, with 400 mm min^{-1}, and z-height of 58 mm. In the "environmental conditions" section, the number represents the starting temperature in Celsius of the dough, a "c" means that the dough was covered with a laser-permeating acrylic, an "s" means that the dough was sealed in contact with a laser-permeating acrylic, a "v" means that the feed rate was decreased to 300 mm min^{-1}, an "rh" means that the relative humidity was increased in the environment. The laser was operating at a z-height of 58 mm, and speed of 400 mm min^{-1} (unless otherwise indicated). In the "repetitive heating" section, the number preceding the "x" denotes the number of circular ring passes that were executed. The laser feed rate was maintained at 4000 mm min^{-1}, at a z-height of 28 mm (focal length). The laser was operating at 2 W for all of these tests.

		Temperature probe depth (°C)			
		0.25 mm		1.0 mm	
		Average	Std error	Average	Std error
Recipe Variance	50% water	87.0	2.2	70.8	1.8
	70% water	106.7	3.3	85.6	3.4
Pattern Exploration	Hilbert	89.1	0.5	70.1	3.9
	Int. Circles	92.6	2.1	74.1	3.5
	Rectangle	50.0	5.4	61.6	2.6
	Spiral	75.9	0.4	63.0	1.6
	Square	95.8	3.5	75.6	1.3
Environmental effects	23	95.8	3.5	75.6	1.3
	40	92.7	5.1	71.8	2.9
	40, c	99.7	4.4	80.4	3.1
	50, c	98.9	1.6	82.0	6.0
	40, s	87.0	7.3	82.1	5.1
	40, s, v	110.1	5.2	86.3	0.1
	40, rh, c	66.6	1.6	71.3	2.9
	40, rh, c, v	78.7	2.2	69.5	3.0
Repetitive heating	100x	70.9	3.0	67.0	1.1
	200x	80.4	2.7	75.3	0.7
	300x	86.5	2.2	79.8	1.0
	400x	88.7	2.2	82.1	0.5
	500x	90.7	2.9	83.5	0.2
	600x	91.0	2.8	84.1	0.2
	700x	91.3	2.7	84.4	0.2
	800x	91.4	2.6	84.6	0.3
	900x	92.7	3.2	84.8	0.4
	1000x	92.7	3.2	84.8	0.4

efficiently within the dough. Third, targeted cooking can be easily controlled by adjusting the direction of motion of the interlaced circles. The feed rate for the square, rectangle, spiral, and Hilbert cooking pattern were identical at 600 mm min^{-1}, while the interlaced circles were cooked at a speed of 3000 mm min^{-1}. These feed rates correspond to a total cook time—in increasing order—of 113 s for interlaced circles, 132 s for spiral, 164 s for Hilbert, 167 s for rectangle, and 173 s for square.

Altering the laser-baking pattern changes the energy profile supplied to the dough, which results in different final baking temperatures (Table 1). Maximum internal dough temperatures (at 0.25 mm and 1.0 mm depth from the dough surface) are very similar for the square, Hilbert, and the interlaced circles cooking patterns (89–96 °C at 0.25 mm depth and 70–76 °C at 1.0 mm from the dough surface). The rectangular raster pattern generates less heat within the dough than the square raster pattern does, since it takes more time to complete a horizontal pass across the specimen. Consequently, the laser has a longer path to travel before it changes direction, giving the dough more time to cool down (Wojtkowiak, 2014). The greater variance in energy supplied to the dough when the rectangular pattern is applied reduces the maximum dough temperature to 50 °C at a depth of 0.25 mm (46 °C lower than that achieved by the square pattern) and 62 °C at a depth of 1.0 mm (14 °C lower than that attained when square pattern is used).

While the temperatures measured inside the dough samples exposed to the square, Hilbert, and interlaced circles cooking patterns are sufficient to initiate the starch gelatinization process (Olkku and Rha, 1978), it remains incomplete, as complete starch gelatinization in bakery products occurs when the temperature inside the dough reaches 96 °C at the minimum (Zanoni et al., 1995a).

3.2.1. Interlaced circles cooking pattern parameterization

To determine the most optimal interlaced circles pattern, circle density and circle diameter were independently varied and assessed the outcome. Fig. 4 show the images of dough samples cooked by varying these two parameters while maintaining the laser at 28 mm distance above the sample surface. The transition of raw to cooked dough (with visible crumbs) can be clearly observed, as it corresponded to dough becoming a lighter color shade (Purlis and Salvadori, 2009).

The experimental results revealed that, when the circle density exceeded 12 rev mm^{-1}, the dough sample was prone to burning. Increased surface absorbance of the laser energy also hinders heat penetration through the dough. This phenomenon can be observed in the bottom view images in Fig. 4, where a darker shade of the dough surface corresponds to a decrease in penetration. At circle densities below 10 rev mm^{-1}, the dough surface is insufficiently cooked, without improvement in penetration depth. Thus, the optimal balance between energy and power density for a circle of 3 mm diameter was achieved at 12 rev mm^{-1}.

Circle diameter also has an important effect on the heating characteristics of the dough sample. One can deduce from Fig. 4 that diameters <3.0 mm result in surface burning due to low variance in laser exposure, whereby the heat builds up rapidly at the surface. Conversely, when the laser moves in a circle of >4.0 mm diameter, it does not deliver enough heat to the sample to effectively cook the dough. Thus, 3.0 mm was determined as the optimal circle density.

While the interlaced circles cooking pattern is great for efficiently heating dough, its geometry makes it difficult to heat the corners of orthogonal shapes due to the fact that it is circular. Multiple approaches can be taken to solve this issue: 1) new interlaced patterns can be produced that consist of interwoven squares with small fillets on each corner as opposed to circles, 2) the relationship between circle diameter, circle density, and feed rate can be further parameterized to use smaller circles that can fit in tighter corners, and 3) inspiration for new cooking patterns can be taken from the manufacturing industry (Pateloup et al., 2004) that optimizes paths for cooking corners.

3.2.2. Energy distinction between baking and burning of dough

During the interlaced circles baking trials (A and B, Fig. 4), overexposure to laser energy caused a few final cooked dough samples to burn rather than bake. Rapid increases in heat with insufficient time for heat to gradually build up in the dough sample can result in burning of the dough. Laser energy per area of dough (ω) was calculated for baked dough samples and burned dough samples to assess the amount of laser energy transfer per unit area (J m^{-2}) required to burn dough. Multiple data points were taken from the interlaced circles cooking test (A and B, Fig. 4) and the corresponding ω values were calculated from Equations (1), (2b) and (5). From that data in Table 2, it can be inferred that an $\omega \geq 1.2$ MJ m^{-2} will result in burning of the dough sample, while baking of dough requires that $0.8\ \text{MJ m}^{-2} < \omega < 1.2\ \text{MJ m}^{-2}$. This analysis only pertains to the interlaced circles cooking pattern but can be extended to other laser-cooking patterns. Furthermore,

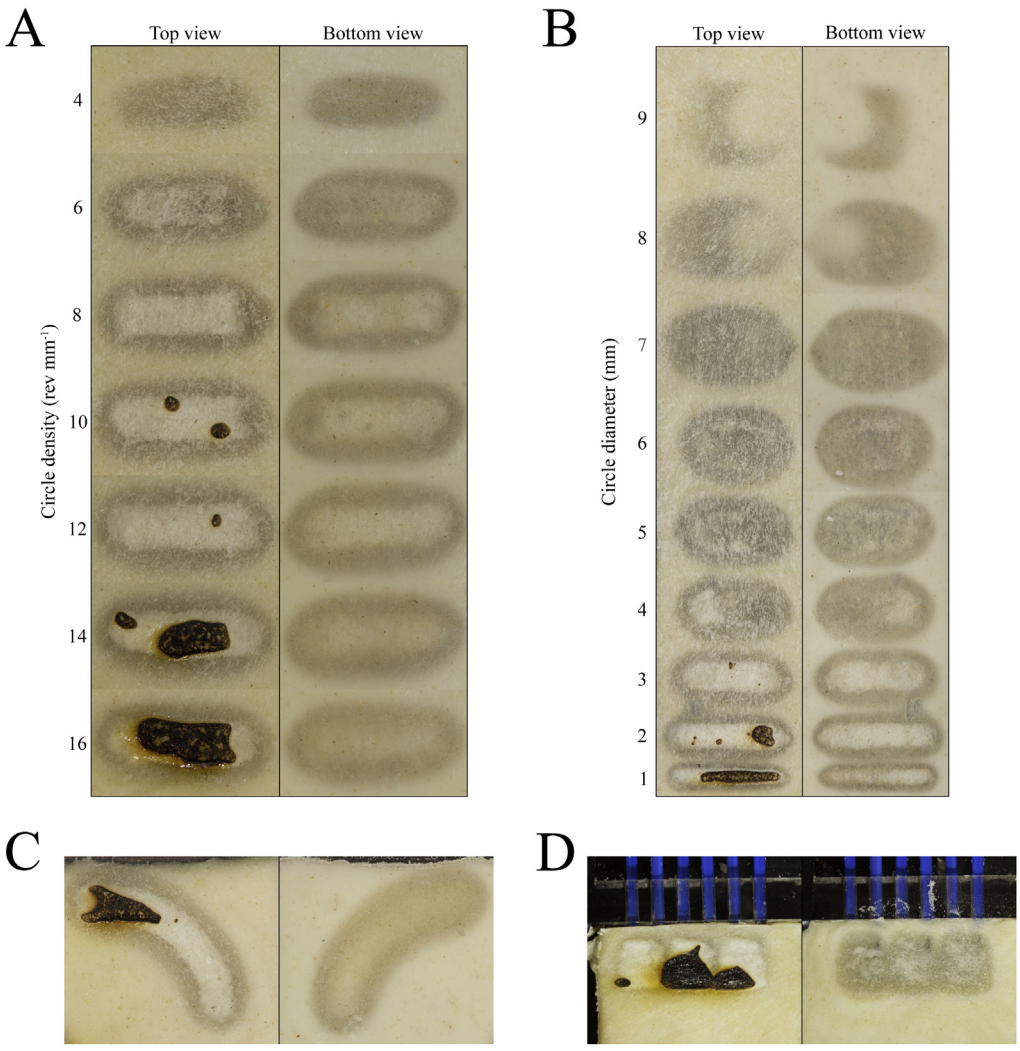

Fig. 4. Effects of changing the circle density and circle diameter when applying the interlaced circles cooking pattern and dough water content. (A) The results obtained when the laser was run at varying circle densities, while keeping the power, speed, and circle diameter (3.0 mm) constant. (B) The outcome of changing the circle diameter, while keeping power, speed, and circle density (10 circles mm^{-1}) constant. The parameters that were held constant in these tests are as follows: speed = 3000 mm min^{-1} and z-height = 28 mm (focal length). (C) Burn propagation during laser-baking of dough. The interlaced circles pattern has a diameter of 3.0 mm, circle density of 15.9 circles mm^{-1}, speed of 3000 mm min^{-1}, and z-height of 28 mm (focal length). As the pattern propagates on an arc towards the upper left (counter-clockwise), the width of the burned region increases from a point to the full width of the interlaced circle diameter. (D) Effects of water content on laser-baked dough temperature. Two dough recipes were prepared: a sample with (left) 50% water on a flour weight basis and (right) 70% water on a flour weight basis. The blue cables feeding into the dough samples had exposed thermistors, which gathered temperature data within the dough at various depths. The parameters held constant during these tests were laser speed (400 mm min^{-1}) and z-height (58 mm). (For interpretation of the references to color in this figure legend, the reader is referred to the Web version of this article.)

Table 2
Calculating laser energy per unit area required to burn and bake dough. The D and ρ values were taken from the interlaced circles cooking pattern trials in Fig. 4. Laser speed (3000 mm min^{-1}), laser power (2 W), and l (10 mm) were constant for all tests.

	D (mm)	ρ (rev mm^{-1})	t_{ic} (s)	E_{laser} (J)	A_{ic} (μm^2)	ω (MJ m^{-2})
Baking	3	8	15.1	30.2	37.1	0.8
	3	10	18.8	37.7	37.1	1.0
	3	12	22.6	45.2	37.1	1.2
	2	10	12.6	25.1	23.1	1.1
Burning	3	14	26.4	52.8	37.1	1.4
	3	16	30.2	60.3	37.1	1.6
	1	10	6.3	12.6	10.8	1.2

when burn marks occurred on the dough surface, they tended to develop after a few circles had already been scanned on the dough surface (C, Fig. 4). This could be due to the fact that the dough is getting dryer due to heat conduction from the baked rings that precede the onset of the surface burning propagation.

3.2.3. Comparing energy delivery efficiency

The efficiency of each laser-cooking pattern was compared for effectiveness of heating using Equations (1), (3) and (4) (from Section 2.3.1). In calculating the heat energy (Q) generated in each dough sample from laser heating, the specific heat capacity of the dough was assumed to be 2760 J kg^{-1} K^{-1} based on temperature and moisture content (Rask, 1989). The laser scanning gap (g) was 0.1 mm and the mass of the heated sample (m) was 0.75 g for the square, rectangle, spiral, and Hilbert cooking patterns. The interlaced circles pattern spanned a slightly larger area on the dough resulting in a total heated mass of 0.78 g. Circle density (ρ) for the interlaced circles pattern was 10 rev mm^{-1}, diameter (D) was 3 mm, and distance traveled (l) was 60 mm.

The interlaced circles cooking pattern yielded the highest heating efficiency (η). In descending order from most effective at heating dough to least effective at heating dough was the interlaced circles (55%), square (38%), Hilbert (37%), spiral (36%), and rectangle (20%). Because the interlaced circles cooking pattern is the only pattern that provides repeat exposure to a voxel of dough during a cooking cycle, and because the laser moves at a much higher speed, there is more time for heat to build up in the dough (Wojtkowiak, 2014). The variance of energy to each voxel of dough during a cooking cycle was much lower for the interlaced circles pattern than it was for the rectangular raster pattern since less time passed between successive laser passes.

3.3. Effect of ambient temperature and moisture on maximum dough temperature

In conventional metal laser sintering, the ambient conditions of the powder bed are set just below the melting temperature (Fabian, 2017), thus reducing the amount of laser energy required to melt the metal to produce 3D objects. Using this principle, the ambient temperature around the dough was increased in an attempt to achieve complete starch gelatinization at a depth of 1.0 mm below the dough sample surface. In the experiments, starting ambient temperature, relative humidity (RH), and evaporative characteristics of the dough were altered (Fig. 5). Table 1 shows the effects of altering the aforementioned environmental factors prior to subjecting the dough to laser heating.

Warming the environment, increasing the relative humidity, and changing the speed at which the cooking pattern is executed were found ineffective in raising the dough temperature in order to achieve complete starch gelatinization (96 °C) at 1.0 mm depth below the sample surface. A test was performed where the laser speed was decreased to 300 mm min^{-1}. Under normal conditions this would cause surface burning, but since the dough samples were sealed by an acrylic cover, moisture evaporation was decreased. The effect of moisture content on browning rates has been studied extensively (Eichner and Karel, 1972; Peterson et al., 1994). While browning doesn't occur during these tests, one can assume that a high moisture content—by sealing the dough with acrylic—with limited oxygen will decrease the possibility of burning. The use of a lower speed also increased the amount of energy supplied to the sample, increasing the maximum temperature to 95 °C, which is significantly higher than the 76–82 °C achieved at 400 mm min^{-1}. The microstructure of the sample heated at 300 mm min^{-1} via SEM was examined, since the internal temperature was very close to that required for complete starch gelatinization (96 °C).

3.3.1. SEM analysis of sealed dough sample

The microstructure produced by heating the sealed dough is characterized by a very dense starch network that becomes hard and brittle after drying (C, Fig. 6). Though starch gelatinization did occur, as can be seen from the interwoven network in the left portion of Fig. 6 (Srivastava et al., 2002), the acrylic cover inhibited network expansion. Consequently, using this method for cooking dough products is not recommended, as it will not yield an acceptable texture. It would also be highly impractical to seal each food layer prior to laser cooking in an FLM application.

The findings indicate that higher speeds and repeated exposure are required for successful laser cooking, as these conditions will allow heat to build up in the sample without burning the surface. Higher laser speeds could also allow for the use of more powerful lasers, which should improve penetration depth as well.

3.4. Effect of energy variance on maximum dough temperature

To achieve complete starch gelatinization—and an internal dough temperature of 96 °C—a dough sample was continuously exposed to a circular ring pattern at high speed. Temperatures in dough were measured at a penetration depth of 0.25 mm and 1.0 mm (Table 1). For the blue diode laser, a 7.5 mm circular ring pattern delivered at a speed of 4000 mm min^{-1} was used, with the laser powered at 2 W positioned at 28 mm distance from the

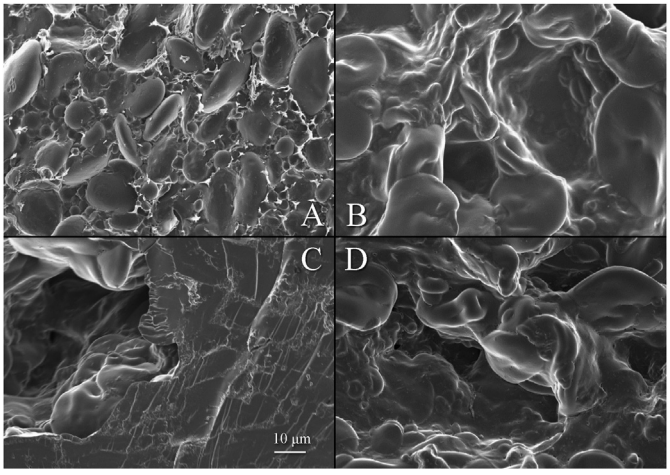

Fig. 6. Microstructure images of dough obtained by SEM: A) raw uncooked, B) blue laser-baked, C) blue laser-baked at 40 °C ambient temperature and sealed with acrylic, and D) oven-baked. The raw dough sample (A) shows intact starch granules. The oven-baked sample (D) was cooked at 220 °C for 5 min. The blue laser-baked dough sample (B) was cooked using 120 repetitions of a ring-shaped pattern delivered at a speed of 4000 mm min^{-1}, from 28 mm height, with 2 W laser power. The sealed blue laser-baked sample (C) was cooked with a 7.5 mm square laser-cooking pattern at a speed of 300 mm min^{-1} and z-height of 58 mm. All images were obtained using a scanning electron microscope at 1000 × magnification. The scale bar corresponds to 10 μm.

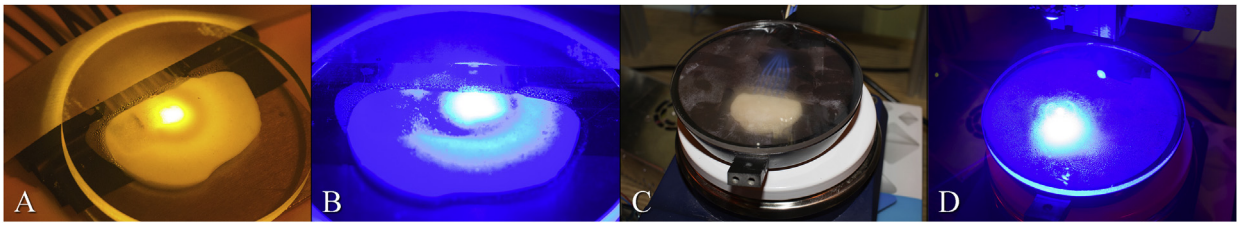

Fig. 5. Studying the effects of changing ambient conditions on the cooking results. Our method of sealing and/or covering the dough sample involved using a transparent acrylic plate, which allowed for the transmittance of blue laser light. We performed tests with sealed dough and raised ambient conditions (A and B), as well as covered dough with raised ambient conditions (C and D). We used a hot plate (visible in C and D) to generate a warmer environment. In C and D, the condensation can be attributed to the water that was left to heat in the enclosed environment around the dough sample, while in A and B the condensation is due to evaporation in the dough due to heating. (For interpretation of the references to color in this figure legend, the reader is referred to the Web version of this article.)

sample. The internal dough temperature approaches thermal equilibrium (Borgnakke and Sonntag, 2013) after about 500 pattern repetitions—as is evident in Table 1. At thermal equilibrium a maximum temperature of 93 °C is obtained just below the dough surface and 85 °C is measured at 1.0 mm below the surface. One can postulate that diffusion and cooling effects prevent the dough from reaching a temperature sufficient to complete the starch gelatinization process. Increased heat buildup and less diffusion are necessary for inducing complete starch gelatinization in a dough sample.

3.5. Effect of dough thickness on heating

To assess the effect of thermal diffusion within the dough, a 1 mm and a 5 mm thick dough sample were exposed to the blue laser while keeping speed, power, z-height, and ambient conditions unchanged. The difference in the final appearance of these two cooked dough samples is shown in Fig. 7. The lighter surface color of the thinner dough sample (C, Fig. 7) indicates a clear transition from raw to cooked dough (crumb-like texture). This transition is not visible, however, in the thicker dough sample (D, Fig. 7), which has a more transparent appearance indicating that it has undergone some heat-related transition but no clear crumb formation (Popov-Raljić et al., 2009).

Dough thickness has a marked effect on the laser-baking process, as it influences the laser beam diffusion and energy dispersion. Because thinner dough products can be baked more efficiently (Açar and Gökmen, 2009), a test was performed in which laser energy was delivered in a repeated circular ring pattern to a 1 mm thick dough sample. The ring diameter was decreased to 5 mm to allow for more concentrated heat buildup. A maximum temperature of 105 °C (±1.5 °C) was achieved inside the dough after 30 repetitions of the ring pattern. The dough sample underwent a clear transition to a crumb-like appearance after 120 repetitions of the ring pattern (Fig. 7). The bottom view of this sample (B, Fig. 7) also shows complete heat penetration through the dough. Significant heat diffusion can be seen in the more transparent dough around the baked ring.

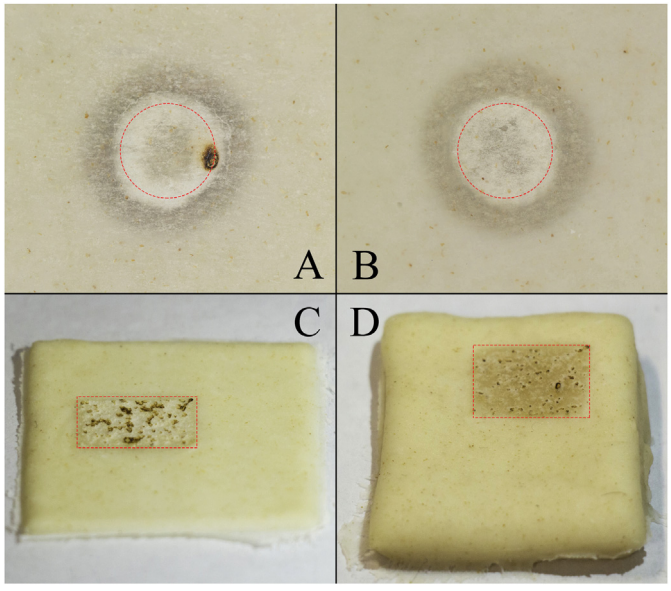

Fig. 7. Effect of repetitive laser exposure (A: top view & B: bottom view) and dough thickness (C: 1 mm & D: 5 mm thick) on laser-baking outcome. We successfully baked a (A & B) 1 mm thick dough sample using a 5 mm ring-shaped cooking pattern, 120 repetitions, 4000 mm min^{-1} speed, 28 mm height, and laser power of 2 W. The (C) thin and (D) thick dough sample were exposed to a rectangular raster pattern with 2 W laser beam delivered at a speed of 700 mm min^{-1} from 40 mm height. In A and B the dashed red line indicates the ring laser-baking pattern, while in C and D the dashed red box indicates the area of the raster pattern. (For interpretation of the references to color in this figure legend, the reader is referred to the Web version of this article.)

3.5.1. SEM analysis of circular ring pattern baked on thin dough sample

The microstructure of dough baked using blue laser is very similar to that of oven-baked dough. The dough microstructure of a raw sample, oven-baked sample, and a blue laser-baked sample was compared by analyzing the corresponding SEM images (Fig. 6). These images indicate that both the blue laser-baked dough sample (D, Fig. 6) and the oven-baked dough sample (B, Fig. 6) have undergone starch gelatinization. The air pockets in the structure also demonstrate a porous network, which is a desirable trait in baked dough products. This network porosity is also confirmed by the visual changes in the dough macrostructure (Srivastava et al., 2002). The final baked dough did show a slight volume increase (Fan et al., 1999).

We demonstrate—by SEM imaging—that dough can be sufficiently heated by a blue laser to generate a texture comparable to that achieved in an oven-baked dough sample. Further sensory tests are needed, however, to determine the acceptance of the laser-baked dough product for human consumption. It is noteworthy that, while blue laser-baking can result in considerable starch gelatinization, no surface browning occurs. Browning is important, since color is often used as an indicator of quality in baked products (Abdullah, 2008). Thus, further processing with an IR laser is required to achieve optimal browning.

4. Conclusions

We demonstrate that blue lasers can facilitate complete starch gelatinization in 1 mm thick dough products. Repeated exposure to blue laser energy at high speeds while allowing sufficient time for heat to increase within the dough samples is the most effective way of achieving the necessary internal dough temperatures. Higher cooking speeds can be achieved with the use of mirror galvanometers (galvo mirrors), an approach that works more effectively in 3D food printer applications since galvo mirrors keep the laser stationary and allow for more innovative cooking patterns. In addition, our microstructure analyses indicate that blue laser-baked and oven-baked dough samples exhibit very similar starch swelling, suggesting equivalent nutrient levels. By altering the water content of the food or the laser-cooking pattern, one can also control the internal temperature, heat penetration, and texture of a final cooked food product. For customized cooking scenarios, a 3D food printing system would combine a blue laser for penetrative heat qualities and an IR laser for surface browning capabilities.

Acknowledgements

This work was supported in part by Columbia University's SEAS Interdisciplinary Research Seed (SIRS) funding program.

References

Abdullah, M.Z., 2008. 20 – quality evaluation of bakery products. In: Computer Vision Technology for Food Quality Evaluation, pp. 481–522. https://doi.org/10.1016/B978-012373642-0.50023-5.

Açar, Ö.Ç., Gökmen, V., 2009. Investigation of acrylamide formation on bakery products using a crust-like model. Mol. Nutr. Food Res. 53, 1521–1525. https://doi.org/10.1002/mnfr.200800585.

Almeida, E.L., Chang, Y.K., 2013. Structural changes in the dough during the pre-baking and Re-baking of French bread made with whole wheat flour. Food Bioprocess Technol. 6, 2808–2819. https://doi.org/10.1007/s11947-012-0926-2.

Borgnakke, C., Sonntag, R.E., 2013. Fundamentals of Thermodynamics. Don Fowley, p. 6.
Eichner, K., Karel, M., 1972. Influence of water content and water activity on the sugar-amino browning reaction in model systems under various conditions. J. Agric. Food Chem. 20, 218–223. https://doi.org/10.1021/jf60180a025.
Fabian, 2017. How Direct Metal Laser Sintering (DMLS) Really Works | 3D Printing Blog | i.materialise [WWW Document]. URL https://i.materialise.com/blog/direct-metal-laser-sintering-dmls/(accessed 8.7.17).
Fan, J., Mitchell, J.R., Blanshard, J.M.V., 1999. A model for the oven rise of dough during baking. J. Food Eng. 41, 69–77. https://doi.org/10.1016/S0260-8774(99)00070-9.
Huang, J., Hess, W.M., Weber, D.J., Purcell, A.E., Huber, C.S., 1990. Scanning electron microscopy: tissue characteristics and starch granule variations of potatoes after microwave and conductive heating. Food Struct. 9, 113–122.
Lipton, J.I., Cutler, M., Nigl, F., Cohen, D., Lipson, H., 2015. Additive manufacturing for the food industry. Trends Food Sci. Technol. 43, 114–123. https://doi.org/10.1016/J.TIFS.2015.02.004.
Mondal, A., Datta, A.K., 2008. Bread baking – a review. J. Food Eng. 86, 465–474. https://doi.org/10.1016/j.jfoodeng.2007.11.014.
Olkku, J., Rha, C., 1978. Gelatinisation of starch and wheat flour starch—a review. Food Chem. 3, 293–317. https://doi.org/10.1016/0308-8146(78)90037-7.
Pateloup, V., Duc, E., Ray, P., 2004. Corner optimization for pocket machining. Int. J. Mach. Tool Manufact. 44, 1343–1353. https://doi.org/10.1016/J.IJMACHTOOLS.2004.04.011.
Peterson, B.I., Tong, C.-H., Ho, C.-T., Welt, B.A., 1994. Effect of moisture content on maillard browning kinetics of a model system during microwave heating. J. Agric. Food Chem. 42, 1884–1887.
Pope, R.M., Fry, E.S., 1997. Absorption spectrum (380–700 nm) of pure water II Integrating cavity measurements. Appl. Optic. 36 (8710). https://doi.org/10.1364/AO.36.008710.
Popov-Raljić, J.V., Mastilović, J.S., Laličić-Petronijević, J.G., Popov, V.S., 2009. Investigations of bread production with postponed staling applying instrumental measurements of bread crumb color. Sensors 9, 8613–8623. https://doi.org/10.3390/s91108613.
Purlis, E., 2012. Baking process design. In: Handbook of Food Process Design. Wiley-Blackwell, Oxford, UK, pp. 743–768. https://doi.org/10.1002/9781444398274.ch26.
Purlis, E., Salvadori, V.O., 2009. Modelling the browning of bread during baking. Food Res. Int. 42, 865–870. https://doi.org/10.1016/j.foodres.2009.03.007.
Rask, C., 1989. Thermal properties of dough and bakery products: a review of published data. J. Food Eng. 9, 167–193. https://doi.org/10.1016/0260-8774(89)90039-3.
Srivastava, A.K., Meyer, D., Rao, P.H., Seibel, W., 2002. Scanning electron microscopic study of dough and chapati from gluten-reconstituted good and poor quality flour. J. Cereal. Sci. 35, 119–128. https://doi.org/10.1006.
Sun, J., Peng, Z., Yan, L., Fuh, J.Y.H., Hong, G.S., 2015. International journal of bioprinting, International Journal of Bioprinting. Whioce.
Wang, S., Copeland, L., 2013. Molecular disassembly of starch granules during gelatinization and its effect on starch digestibility: a review. Food Funct 4 (1564). https://doi.org/10.1039/c3fo60258c.
Wojtkowiak, J., 2014. Lumped thermal capacity model. In: Encyclopedia of Thermal Stresses. Springer Netherlands, Dordrecht, pp. 2808–2817. https://doi.org/10.1007/978-94-007-2739-7_393.
Zanoni, B., Peri, C., Bruno, D., 1995a. Modelling of browning kinetics of bread crust during baking. LWT - Food Sci. Technol. (Lebensmittel-Wissenschaft -Technol.) 28, 604–609. https://doi.org/10.1016/0023-6438(95)90008-X.
Zanoni, B., Schiraldi, A., Simonetta, R., 1995b. A naive model of starch gelatinization kinetics. J. Food Eng. 24, 25–33. https://doi.org/10.1016/0260-8774(94)P1605-W.
Zoran, A., Coelho, M., 2011. Cornucopia: the Concept of Digital Gastronomy, vol.44, pp. 425–431.